Compact Active EMI Filter for Reduction of CM Conducted Emission in High Power System Implemented by the Integrated Circuit

Sang Yeong Jeong[1], Jun Sik Park[2] and Jin Gook Kim[a]
[1]School of ECE, Ulsan National Institute of Science and Technology
[2]Samgsung Electronics.
E-mail : [1]jsy9121@unist.ac.kr, [2]pjs3300@unist.ac.kr

***Abstract* - This paper proposes the integrated circuit (IC) within the active EMI filter (AEF). The fully-isolated feed-forward current-sense current-compensation (CSCC) structure of the AEF is also proposed to achieve the robust reliability from electromagnetic susceptibility (EMS) to the designed IC. The noise attenuation performance is analyzed, and the design guides for the proposed AEF with IC are developed. The designed IC is fabricated by 180nm BCD process. The noise attenuation performance and stability are experimentally validated by vector network analyzer (VNA) measurement.**

Keywords—Active EMI filter (AEF), Bipolar-CMOS-DMOS (BCD) process, Conducted Emission (CE), Electromagnetic interference (EMI), Integrated Circuits (ICs)

I. INTRODUCTION

Electromagnetic interference (EMI) filter is one of the essential components in the recent power electronics system to suppress the EMI noise caused by high-speed switching operation. Among various EMI noise regulations, the conducted emissions (CEs) are most related issues for the design of an EMI Filter. Most of the power systems include the EMI filter at the ac grid. The noise attenuation performance of an EMI filter should be sufficiently high to suppress the EMI noise under the regulated noise level which is specified in CISPR or FCC standard [1]-[2].

The traditional EMI Filter usually consists of reactive passive components such as X-capacitors, Y-capacitors, and common-mode (CM) chokes [3]-[4]. To increase noise attenuation performance, the value of capacitors and inductance of the CM chokes should be sufficiently large. However, the capacitance of Y-capacitors is limited by safety regulation considering the electric shock to human body [3]. In case of the X-capacitor, there is a limit to the overall noise reduction because it cannot directly reduce the CM noise. In addition, if the capacitance of X-capacitors increases arbitrarily, it can adversely affect the performance of the ac-line power stage such as power factor [4]. As a result, the inductance of the CM choke should increase for the several practical reasons. However, CM chokes become bulky and costly in high power system to avoid the magnetic saturation and heat problems.

To overcome the cost and size limit of the traditional passive EMI filter, the active EMI filters (AEFs) has been suggested to effectively reduce the CE noises without significant increase of the filter size in a high-power system by employing active circuit components [5]-[8]. When the AEF product is applied to a real power electronics product, mass production is necessary to satisfy the demand of various individual and industrial products as the traditional passive EMI filter has been. Therefore, the huge amount of semi-conductor devices should be manufactured and supplied to comprise the AEFs. The presented AEF researches employed the commercial discrete semi-conductor devices such as OP-amp, bipolar junction transistors (BJTs) pair, and digital signal processor (DSP) hardware. However, for considering the mass-production, the active parts employing the integrated circuits (ICs) can be the most economical and the smallest method to implement the AEFs as many electronic products has been. In addition, optimized performance of the semi-conductor devices can be achieved by full-custom IC design.

This paper proposes the AEF employing the full-custom IC with considering the high-voltage transient and even in high EMI noise environment for the high-power system. In Section II, basic structure and design guidelines for the proposed AEF using ICs are introduced and analyzed. Based on the analyzed AEF structure, the integrated active circuit parts and nearby components are designed, considering the required design conditions in Section III. In Section IV, the noise attenuation performance and loop gain of the AEF are validated by measurements using a vector network analyzer (VNA). The reduction of the CM CE noise by the AEF is also demonstrated with a real product power system.

a. Corresponding author; jingook@unist.ac.kr

Manuscript Received Oct. 30, 2020, Revised Dec. 11, 2020, Accepted Dec. 21, 2020

II. A BASE CIRCUIT BLOCK OF DESIGNED ACTIVE EMI FILTER

The circuit model of the proposed AEF is described in Fig. 1. The CM noise source of the equipment under test (EUT) is modeled as the Thevenin equivalent circuit, V_n and Z_n. The AEF is mainly composed of the sensing transformer, the amplifier part, and the compensation capacitor with injection transformer. The turn ratio of the winding on a power line to the sensing winding is set as $1{:}N_{sen}$, and self-inductance of each winding is given as L_{sen} and $N_{sen}^2L_{sen}$, respectively. Likewise, the turn ratio of the primary winding to secondary winding at injection transformer is set as $1{:}N_{inj}$, and self-inductance at each side is then given as L_{inj} and $N_{inj}^2L_{inj}$. At the noise compensation part, noise compensation current is injected through C_{inj}. C_Y are also additionally installed on power lines to satisfy the impedance condition of maximum AEF performance, when the AEF is installed with other EMI filter components such as a CM choke.

The amplifier part is implemented by the BJT push-pull amplifier. C_b and C_e represent the ac-current bypassing capacitors at the bases and emitters of BJTs. R_{npn}, R_{pnp}, R_{bb}, and R_e are implemented to design the DC operating point of BJTs, and the amplifier is designed as a class-AB amplifier. C_{DC} represents a decoupling capacitor for the V_{DC} power supply, and it also provides an ac coupling path between each collector node of *npn* and *pnp* BJTs. Since the amplifier part is fully transformer-isolated from the power lines and earth ground, low-voltage rating circuit components in the AEF can operate at any different reference voltages from the earth ground, which provides an important design freedom in the dc-supply voltage for the AEF.

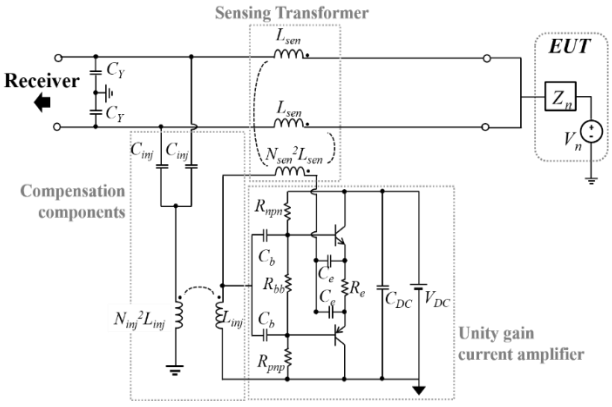

Fig. 1. Circuit model of the proposed AEF

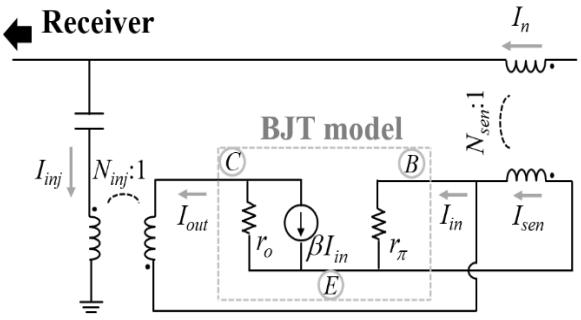

Fig. 2. Simplified half-portion small-signal model

Fig. 2 shows the simplified small-signal model of the proposed AEF. By symmetry of the circuit structure, only half portion of the circuit components are represented, and parasitic components are not considered for simple analysis. The *npn* BJT is represented by small-signal model, where β, r_π, and r_o represent current gain, base resistance, and output resistance of the BJT. As shown in Fig. 2, the sensing transformer senses the noise current flowing through windings on power lines, I_n, and sensing current, I_{sen}, is injected to the input of BJT amplifier. In addition, output current from the BJT, I_{out}, flows through the injection transformer and returns to the base of the BJT. Thus, the BJT amplifier comprises the shunt-series feedback structure, and the closed-loop current gain of the BJT amplifier is solved using feedback theory as

$$\frac{I_{out}}{I_{sen}} \approx -\frac{\beta}{1+\beta} \approx -1 \tag{1}$$

where r_o is sufficiently higher than impedance looking in to the injection transformer, and this condition usually holds for the most commercial BJTs. The current gain of the BJT, β, is usually much higher than 10, then I_{out}/I_{sen} is close to -1 as shown in (1). Thus, the BJT amplifier works as unity gain current amplifier.

The current gain of the sensing transformer, I_{sen}/I_n, is approximately close to $-1/N_{sen}$, and current gain of the injection transformer, I_{inj}/I_{out}, is $1/N_{inj}$ from Fig. 2. Therefore, to maximize noise attenuation performance by using the AEF, the total closed-loop current gain of the proposed AEF, I_{inj}/I_n, should be designed as

$$\frac{I_{inj}}{I_n} \approx \frac{1}{N_{sen}N_{inj}} = 1 \tag{2}$$

Thus, if the condition of (2) holds by design of N_{sen} and N_{inj}, CM noise current from the EUT, I_n, flows through the earth ground, and current flowing to the noise receiver can be effectively mitigated.

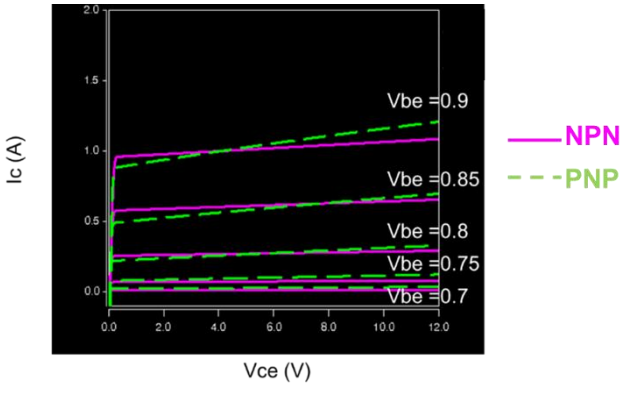

Fig. 3. NPN and PNP device characteristic design and simulation for current amplifier.

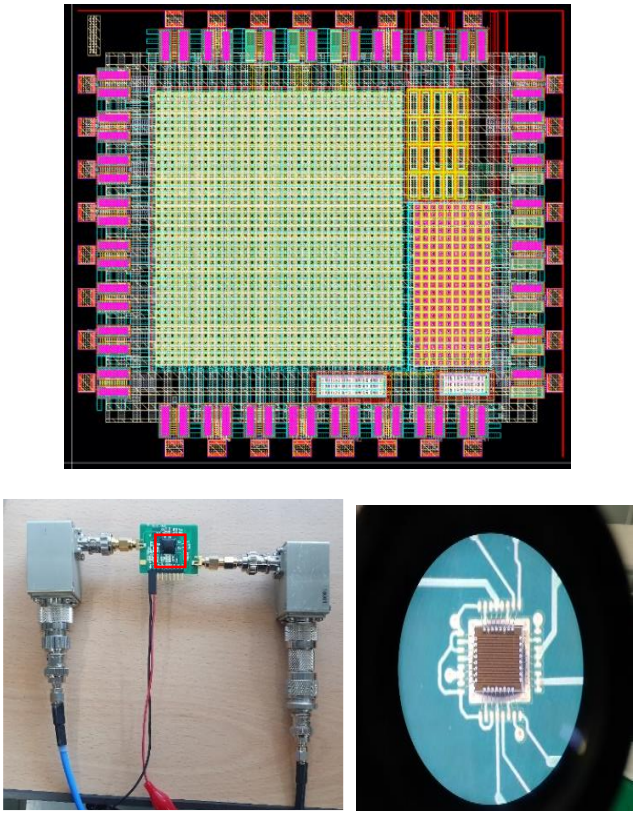

Fig. 6. IC sample Implemented in the AEF test PCB module

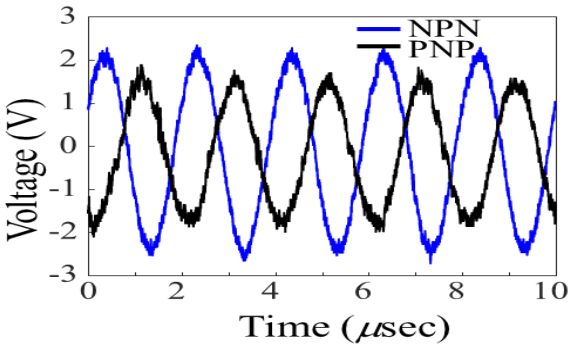

(a)

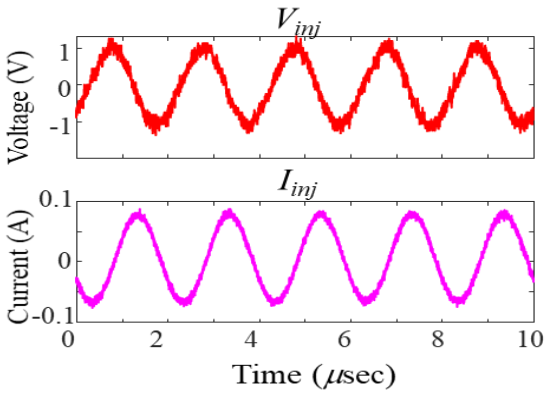

(b)

Fig. 7. Output waveform of BJT current amplifier; (a) Collector-Emitter voltage and (b) injection voltage and current

Fig. 7 shows the implemented IC test set-up for the active EMI filter. The insertion loss (*IL*) of the filter is measured by using vector network analyzer (VNA). The detail port condition and analytical expression for extraction are explained in [9]. A CM choke of 3mH was also implemented at the side of the LISN, where the CM filter comprises the L-C topology because the proposed AEF works as a boosted Y-capacitor at frequency bandwidth of CE regulation. The *IL* of the CM filter with the AEF is compared to those with only Y-capacitors of C_{inj}. Measured results are also compared with simulation results and it shows good agreement. The additional *IL* at 150kHz, which is the lowest frequency of typical CE test, is 14dB, and the AEF achieves the additional *IL* up to 30dB at a frequency range lower than 3Mhz. Although *IL* at over 4Mhz slightly decreases compared with the CM filter without AEF, the proposed AEF effectively reduce the low-frequency CE noises at frequency range from 150kHz to 3Mhz, which can effectively relieve the burden of the CM choke design. In Fig. 7, waveform of the voltage and current were measured by oscilloscope and it shows that the current was well compensated to the injection transformer.

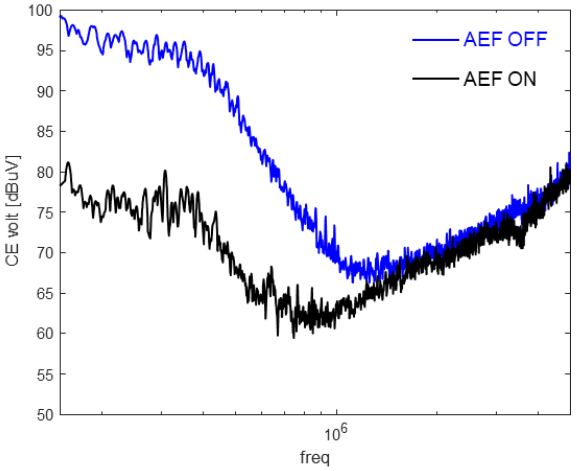

Fig. 8. CE noise reduction by using implemented active EMI Filter IC module.

The reduction of the CM CE noises by utilizing the proposed AEF is demonstrated a 3.3kW real product power system of an inverter motor. Fig. 8 shows the configuration of CE measurement set-up of the target system. CM noise source model includes the compressor, fan motor, inverter, and converter. CM CE noises are measured by using line impedance stabilization network (LISN), CM/DM noise separator, and spectrum analyzer. The designed AEF was routed at ac input of internal printed circuit board (PCB). The ac input of the PCB is connected to the external terminal block by wires about 30cm and connected to each live and neutral lines of the ac power cable. The ground of the AEF is also connected to the chassis of the equipment under test (EUT) by wires of about 30cm to provide the ground connection. Live and neutral line of the cable are connected to the ac input of the terminal block.

Fig. 8 shows the CM CE measurement results with the proposed AEF. For a fair comparison of effective AEF performance, a CE measurement result with Y-capacitor is also compared, where the AEF is replaced by only Y-

capacitors with the same values as those used in the AEF. The CM CEs with the AEF shows a better reduction than with Y-capacitors by 16dB to 20dB in the frequency range from 150kHz to 3MHz.

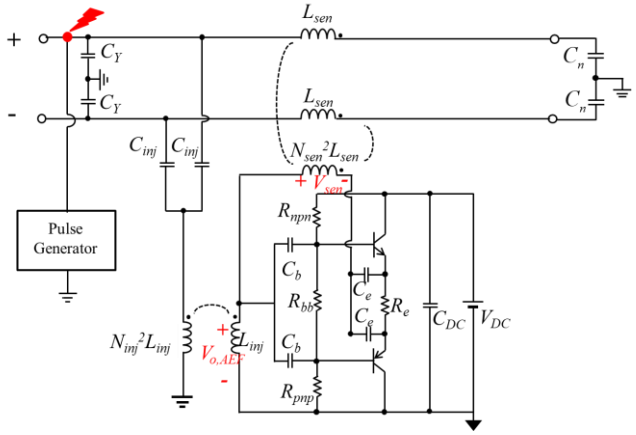

Fig. 9. Surge test setup of the transformer-isolated AEF with TVS diodes installed.

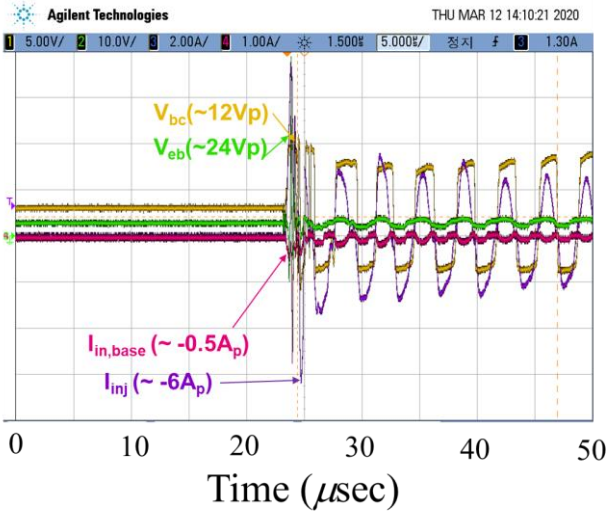

Fig. 10. The voltage waveform measured during the 5kV surge test.

A transformer-isolation also have advantage to the surge immunity, and it is also widely utilized in power electronics application such as flyback converter and the current sensor module. To verify the surge immunity of the proposed transformer-isolated CSCC AEF, surge tests have been performed to an implemented transformer-isolated CSCC AEF, and the test setup is shown in Fig. 9. The 5kV tests have been performed for the target AEF, because the varistor and arrestor in front of the EMI filter can block the voltage above 4kV for the typical surge protection design in a power converter application. The chip-type bidirectional TVS diodes, T_1 and T_2, are implemented at the side of the AEF input and output as shown in Fig. 8. The breakdown voltage of T_1 and T_2 are designed as 12V and 3.5V, respectively, considering the voltage swing for the normal operation of the AEF.

When the TVS diode is used for the surge protection, the junction capacitance of the TVS diode is also an important design factor of the protection circuit design. Even a few hundred-pF capacitances can degrade the AEF performance [10]. The small chip-type TVS diode have usually very low value of junction capacitance such as a few pF as well as its compact size, but the maximum acceptable energy is relatively low for the surge protection and it is usually utilized for the ESD protection. However, in case of the transform-isolated AEF, both peak level and pulse duration of the injected voltage is much reduced by the transformer-isolation at the noise compensation part and noise sensing part. Therefore, the small chip-type TVS diodes can be utilized for the surge protection design at the transformer-isolated AEF.

Fig. 10 shows the measured waveform. The maximum voltage peak of the V_{bc} and V_{eb} limited by 12V and 24V, respectively, due to the voltage clamping of the TVS diodes during the current flow at the diodes. The 20 times of 5kV surge tests have been performed to the target AEF, and no failure had been detected during the tests.

TABLE I. Comparison with Other AEF Researches

	VSVC AEF by Ogasawara [11]	CSCC AEF by Son [12]	This work
Sensing-Injection	Capacitive sensing, Inductive injection	Capacitive sensing, Inductive injection	Capacitive sensing, Inductive injection with transformer
Amp	Commercial BJTs	Commercial BJTs	Customized IC (180nm BCD)
ATT_{max} [dB]	20	20	20
EUT [kW]	3.7	3.7	3.3
Feature	Transformer, Active components dependent	Transformer, Active components dependent	Customized IC used, fully transformer-isolated with high reliability

The feature of the proposed AEF with customized IC is compared with other AEF researches in Table I. There have been several researches realizing the AEF with commercial semiconductor devices, but it is believed that this work is first attempt to implement the AEF with customized IC. The high reliability has been achieved by proposed fully transformer-isolation structure even the semiconductor of low-voltage rating has been used. The noise attenuation performance of the proposed AEF and target EUT is comparable with the AEF implemented by commercial devices. Thus, this work helps to achieve the high stability of the AEF by IC implementation from previous AEF researches.

IV. Conclusions

Transformer-isolated feedforward CSCC AEF has been proposed. The proposed AEF has been estimated by circuit analysis, and a simple design guide has been developed. The amplifier part is implemented by the customized IC, where the designed IC is fabricated by 180nm BCD process. The noise

attenuation performance has been validated with the simulation results and VNA measurements. The proposed AEF effectively reduce the CE noises up to 20dB at frequency range from 150kHz to 3Mhz, which can relieve the burden of the CM choke design. Moreover, the proposed AEF is fully isolated so that the internal low supply voltage in the power system can be available from the control board of the main power system with low risk of EOS and EMS problems. As a further work, the noise attenuation performance of the transformer-isolated AEF will be improved by adjusting the accuracy of the amplifier gain.

ACKNOWLEDGEMENT

The chip fabrication was supported by the IC Design Education Center (IDEC), Korea.
This work was jointly supported by National Research Foundation of Korea (NRF) grant (No. NRF-2020R1A2C1005576) and Institute of Information & communications Technology Planning & Evaluation (IITP) grant (No. 2020-0-00839) both funded by the Korea government (MSIT).

REFERENCES

[1] C. Paul, Introduction to Electromagnetic Compatibility, 2nd ed, John Wiley & Sons, 2006.

[2] K. Mainali, R. Oruganti., "Conducted EMI mitigation techniques for switch-mode power converters: a survey," *IEEE Trans.Power Electron.*, vol.25, no.9, pp.2344-2356, Sept. 2010.

[3] Y. Chu, S. Wang, and Q. Wang, "Modeling and stability analysis of active/hybrid common-mode EMI filters for DC/DC power converters," *IEEE Trans. Power Electron.*, vol. 31, no. 9, pp. 6254–6263, Sep. 2016.

[4] P. Paipodamonchai, "A study of an active EMI filter for suppression of leakage current in motor drive systems," *2015 18th International Conference on Electrical Machines and Systems (ICEMS)*, Pattaya, 2015, pp. 1976-1982.

[5] S. Jiang, Y. Liu, W. Liang, J. Peng and H. Jiang, "Active EMI Filter Design With a Modified LCL-LC Filter for Single-Phase Grid-Connected Inverter in Vehicle-to-Grid Application," *in IEEE Transactions on Vehicular Technology*, vol. 68, no. 11, pp. 10639-10650, Nov. 2019

[6] Y. Zhang, Q. Li and D. Jiang, "A Motor CM Impedance Based Transformerless Active EMI Filter for DC Side Common-Mode EMI Suppression in Motor Drive System," *in IEEE Transactions on Power Electronics*.

[7] B. Narayanasamy and F. Luo, "A Survey of Active EMI Filters for Conducted EMI Noise Reduction in Power Electronic Converters," in *IEEE Transactions on Electromagnetic Compatibility*, vol. 61, no. 6, pp. 2040-2049, Dec. 2019,

[8] L. Dai, W. Chen, Y. Yang, R. Wang and X. Yang, "Design of Active EMI Filters with the Integrated Passive Component," *2019 IEEE Applied Power Electronics Conference and Exposition (APEC)*, Anaheim, CA, USA, 2019, pp. 640-643

[9] S. H. Voldman, "Electrical Overstress (EOS): Challenges for component and system-level co-design," *2015 IEEE 11th International Conference on ASIC (ASICON)*, Chengdu, 2015, pp. 1-4.

[10] S. Jeong, D. Shin, J. Kim, S. Kim and J. Kim, "Design of effective surge protection circuits for an active EMI filter," *2017 Asia-Pacific International Symposium on Electromagnetic Compatibility (APEMC)*, Seoul, 2017, pp. 210-212.

[11] S. Ogasawara, H. Ayano, and H. Akagi, "An active circuit for cancellation of common-mode voltage generated by a PWM inverter," *IEEE Trans. Power Electron*., vol. 13, no. 5, pp. 835–841, Sep. 1998.

[12] Y. Son, S. Sul, "A new active common-mode EMI filter for PWM inverter," *IEEE Trans. Power Electron*, vol. 18, no. 6, pp. 1309-1314, Nov. 2003.

Sang Yeong Jeong received the B.S. degree in electrical engineering from the Ulsan National Institute of Science and Technology, Ulsan, South Korea, in 2015, where he is currently pursuing the Ph. D. degree. His current research interests include electromagnetic compatibility (EMC) problems in the power system and the noise reduction techniques by using integrated circuits (ICs).

Jun Sik Park received the B.S. and Ph.D. degrees in electrical engineering from the Ulsan National Institute of Science and Technology, Ulsan, South Korea, in 2014 and 2019, respectively. He is currently with the Memory business of Samsung electronics, Hwasung, South Korea. His current research interests include electrostatic interference and electrostatic discharge in both component-level and system-level.

Jin Gook Kim (M'09-SM'15) received his B.S., M.S., and Ph.D. degrees in electrical engineering from Korea Advanced Institute of Science and Technology, Daejon, Korea, in 2000, 2002, and 2006, respectively. From 2006 to 2008, he was with DRAM design team in Memory Division of Samsung Electronics, Hwasung, Korea, as a senior engineer. From January 2009 to July 2011, he worked for the EMC Laboratory at the Missouri University of Science and Technology, Missouri, USA, as a postdoc fellow. In July 2011, he joined the Ulsan National Institute of Science and Technology (UNIST), Ulsan, Korea, where

he is currently a professor. His current research interests include EMC, ESD, RF interference, and analog circuits design.